

- air cylinder under a pressure of ~1.5 bar controlled by air lines external to the impact chamber.
13. A. L. Ruoff, *J. Appl. Phys.* **38**, 4976 (1967).
 14. Relaxation times in liquids are strongly dependent on the liquid viscosity. For an alkali olivine basalt at 1300°C and 1 atm, relaxation times are inferred to be <2 nsec [C. S. Rai, M. H. Manghnani, K. W. Katahara, *Geophys. Res. Lett.* **8**, 1215 (1981)] and viscosity η is inferred to be ~55 poises (calculated from the data of Y. Bottinga and D. F. Weill [*Am. J. Sci.* **272**, 438 (1972)]. At 1400°C, $\eta \sim 35$ poise for $\text{An}_{0.36}\text{Di}_{0.64}$. If the relaxation time is <2 nsec, the ultrasonically measured 1-atm bulk modulus should represent the relaxed value. Good agreement with the shock bulk modulus suggests that we also measure the relaxed value in our experiment.
 15. R. Jeanloz and A. B. Thompson, *Rev. Geophys. Space Phys.* **21**, 51 (1983).
 16. H. S. Waff, *Geophys. Res. Lett.* **2**, 193 (1975).
 17. S. K. Sharma, D. Virgo, B. Mysen, *Am. Mineral.* **64**, 779 (1979).
 18. E. Ohtani, F. Taulelle, C. A. Angell, in preparation.
 19. A. Boettcher, Q. Guo, S. Bohlen, B. Hanson, *Geology* **12**, 202 (1984).
 20. The application of our results to complex, natural liquid compositions is, we believe, justified in view of the weak dependence of elastic properties of silicate melts on bulk composition observed in ultrasonic experiments (2, 5).
 21. E. Stolper, *Contrib. Mineral. Petrol.* **74**, 13 (1980).
 22. E. G. Nisbet and D. Walker, *Earth Planet. Sci. Lett.* **60**, 105 (1982).
 23. The Birch-Murnaghan adiabats shown are for magnesian olivine (90 mole percent forsterite), orthopyroxene (90 mole percent enstatite), and mantle garnet [ρ from F. R. Boyd and R. H. McCallister, *Geophys. Res. Lett.* **3**, 509 (1976)] at an initial temperature of 1400°C. Elastic properties, ρ and thermal expansivity for olivine and orthopyroxene are from Jeanloz and Thompson (15); for garnet, the data of N. Soga [*J. Geophys. Res.* **72**, 4227 (1967)] and B. J. Skinner [*Geol. Soc. Am. Mem.* **97**, 75 (1966)] were used.
 24. PREM (Preliminary Reference Earth Model): A. M. Dziewonski and D. L. Anderson, *Phys. Earth Planet. Inter.* **25**, 297 (1981). PEM (Parameterized Earth Models): A. M. Dziewonski, A. L. Hales, E. R. Lapwood, *ibid.* **10**, 12 (1973). Density model from free oscillations: T. H. Jordan and D. L. Anderson, *Geophys. J. R. Astron. Soc.* **36**, 411 (1975).
 25. Z. N. Zharkov and V. P. Trubitsyn, in *Physics of Planetary Interiors*, W. B. Hubbard, Ed. (Pachart, Tucson, 1978), vol. 6, pp. 335 and 338.
 26. Typical estimates of Mg/(Mg + Fe) (molar) for Earth are 0.9 [for example, Basaltic Volcanism Study Project, *Basaltic Volcanism on the Terrestrial Planets* (Pergamon, New York, 1981)]. Recent chemical analyses made by Venera 13 and Venera 14 suggest strong similarities between Venusian and terrestrial surface rocks [V. L. Barsukov *et al.*, *Geochem. Int.* **19** (No. 4), 1 (1982)] and lead us to use a similar internal composition for Venus.
 27. Estimates of Mg/(Mg + Fe) (molar) in Mars and the composition of model Mars magma were taken from T. R. McGetchin and J. R. Smyth [*Icarus* **34**, 512 (1978)]. The initial ρ of model Mars basalt is slightly higher (~2.77 g/cm³) than primitive terrestrial basalt because of higher iron content. However, mantle ρ is inferred to be on the order of 0.2 g/cm³ higher on Mars up to a pressure of ~125 kbar because of the mantle's higher iron content [see the Basaltic Volcanism Study Project (26)]. Thus the pressure at which $\Delta\rho \rightarrow 0$ for Mars would be expected to be higher than on Earth or Venus.
 28. The composition of a primitive lunar magma, a supposed parent to the lunar crust, was taken from A. E. Ringwood, *Origin of the Earth and Moon* (Springer, New York, 1979). An inferred lunar density-depth profile is given in the Basaltic Volcanism Study Project (26).
 29. F. R. Boyd, J. L. England, B. T. C. Davis, *J. Geophys. Res.* **69**, 2101 (1964).
 30. G. A. Lyzenga *et al.*, *ibid.* **88**, 2431 (1983).
 31. The 1-atm ρ of MgSiO₃ liquid is calculated by extrapolation of ρ measurements of J. W. Tomlinson, M. S. R. Haynes, and J. O'M Bockris [*Trans. Faraday Soc.* **54**, 1822 (1958)].
 32. For MgSiO₃ perovskite $K_2^0 = 2620$ kbar and $K_3^0 = 4$ (15). A third-order Birch-Murnaghan equation of state was used in calculating high-pressure ρ values and a thermal expansion, $\alpha = (0.2367 \times 10^{-4}) + (0.5298 \times 10^{-8} T) - 0.5702 T^{-2} K^{-1}$ [H. Watanabe, in *High Pressure Research in Geophysics*, S. Akimoto and M. H. Manghnani, Eds. (Center for Academic Publications, Tokyo, 1982), p. 450], was assumed.
 33. S. M. Stishov, *Sov. Phys. Usp.* **17**, 625 (1975).
 34. E. Ohtani, *Phys. Earth Planet. Inter.* **33**, 12 (1983).
 35. N. H. Sleep, *J. Geol.* **87**, 671 (1979).
 36. J. D. Bass and D. L. Anderson, *Geophys. Res. Lett.* **11**, 229 (1984); H. Sawamoto, D. J. Weidner, S. Sasaki, M. Kumazawa, *Science* **224**, 749 (1984).
 37. We are grateful to L. T. Silver for use of the Lepel radio-frequency generator and for his continued interest. We have benefitted from discussions with and comments from D. L. Anderson, J. D. Bass, A. Boettcher, I. S. E. Carmichael, H. Eissler, R. Hill, M. H. Manghnani, S. A. Morse, O. Navon, R. O'Connell, E. Ohtani, F. Richter, M. L. Rivers, D. R. Scott, D. J. Stevenson, and D. Walker. Supported by NSF grant EAR80-18819. Contribution No. 4112, Division of Geological and Planetary Sciences, California Institute of Technology.

11 June 1984; accepted 10 July 1984

The Oceanic Carbonate System: A Reassessment of Biogenic Controls

Abstract. Fluxes of biogenic carbonates moving out of the euphotic zone and into deeper undersaturated waters of the North Pacific were estimated with free-drifting sediment traps. Short-duration (1 to 1.5 day) sampling between 100 and 2200 meters points to a major involvement in the oceanic carbonate system by a class of organisms which had been relegated to a secondary role—aragonitic pteropods. Pteropod fluxes through the base of the euphotic zone are almost large enough to balance the alkalinity budget for the Pacific Ocean. Dissolution experiments with freshly collected materials shed considerable light on a mystery surrounding these labile organisms: although plankton collections from net tows almost always contain large numbers of pteropods, these organisms are never a major component of biogenic materials in long-duration sediment trap collections. Their low abundance in long-duration collections results from dissolution subsequent to collection. Short-duration sampling showed significant increases in the ratio of calcitic foraminifera to aragonitic pteropods in undersaturated waters, indicating the more stable mineralogic form, calcite, was preserved relative to aragonite. Approximately 90 percent of the aragonite flux is remineralized in the upper 2.2 kilometers of the water column.

The oceans constitute a substantial reservoir for anthropogenic CO₂ (1). The behavior of this reservoir, including its internal physical and chemical processes, is expected to significantly influence the rate of atmospheric CO₂ buildup and thereby the earth's future climate (2, 3). In light of this expectation, the marine CO₂ system has been extensively investigated. Field and laboratory investigations (4–7) have provided a detailed picture of the oceanic distributions of total CO₂, dissolved carbonate ions, and the saturation state of particulate carbonates. Nevertheless, important facets of the marine CO₂ system remain poorly understood. Little is known about the rate of removal of CO₂ from the surface ocean via biogenic particulate carbonates and about the delivery rates of these materials to the undersaturated deep ocean.

For the Pacific Ocean, which constitutes approximately one-third of the earth's total area, there is an extreme paucity of carbonate flux data. Published data include information obtained at a single station in the central Pacific (8, 9), and at another station in the western North Pacific (10). With an unusually shallow carbonate saturation horizon (11) and an alkalinity anomaly in intermediate and deep water attributable to the dissolution of biogenic carbonates

(12), particulate carbonates take on special importance in the Pacific Ocean.

The feature that makes carbonate fluxes in the Pacific of special interest also complicates the interpretation of flux measurements. Dissolution of sedimenting aragonite particulates in the water column begins at relatively shallow depths (11) and generally proceeds rapidly below 100 m (13). As a consequence, long-duration sediment-trap deployments can seriously underestimate the mass fluxes of labile carbonates. In order to minimize this problem, our free-drifting sediment traps were deployed for less than 40 hours. This sampling period, quite brief compared to the deployment times in earlier investigations (8–10), permitted the deployment of numerous sediment traps along an extensive section of the western Pacific (Fig. 1).

The vertical fluxes of particulate matter were estimated with free-drifting sediment traps (cross sectional area, 0.66 m²) patterned after the cone design of Soutar *et al.* (14). In our system, trapped materials are concentrated in a Teflon receptacle (2.5 cm in diameter) at the bottom of the trap's cone (15). Prior to retrieval, the Teflon cup and its contents were isolated from further inputs by a double-ball valve seal activated by an electronic release.

The total particle flux was determined

gravimetrically. Immediately after recovery, particulate materials from the respective traps were filtered onto tared (47 mm in diameter) Nuclepore membranes and then briefly rinsed with distilled-deionized water. The filters were stored in a vacuum desiccator with silica gel until they could be weighed on a microbalance in a shore-based clean facility. Pteropods and foraminifera were identified microscopically, removed from the samples, and transferred to tared Nuclepore membranes with a small nylon brush. To minimize sample contamination, the microscopic examination and transfers were made in a vertical-flow clean bench. After desiccation under vacuum, the biogenic materials were weighed on a microbalance housed in a clean room.

Pteropod fluxes are shown in Fig. 2 as a function of depth for the seven stations on our transect. Because of the influence of saturation state on dissolution rate (16), aragonite saturation horizons are included in Fig. 2. The physical variables used to define the CO₂ system, pH, alkalinity, total CO₂, temperature, salinity, and saturation state are discussed elsewhere (11).

No visibly motile pteropods were included in our mass flux determinations. Moreover, poison, which would have killed any pteropods entering the collection cup, was not used. Furthermore, large, rapid swimmers such as *Cuvierina columnella*, which could have swum into our traps, were excluded from our flux measurements. Thus the only pteropods included in our flux estimates (Fig. 2) are small, abundant species such as *Limacina bulimoides*, *L. inflata*, *L. helicina*, and the juveniles of these and other species. Because of the exclusion of substantial large pteropod masses, we regard our aragonite fluxes as conservative, lower-bound estimates. The average pteropod contributions to mass flux along our transect as a function of depth are as follows: 100 m, 24 ± 8 percent; 400 m, 8 ± 5 percent; 900 m, 5 ± 5 percent; 2200 m, 6 ± 4 percent. Substantial differences in pteropod species composition noted on our north-south transect were consistent with earlier reports for the Pacific (17).

Major variations in the standing crops of organisms such as pteropods are expected over short distance scales, based on biological studies in the open Pacific (18). The data points from the 400-m horizon (Fig. 2) were derived from separate free-drifting sediment traps that were separated by about 1 nautical mile and deployed for the same period of time. The pteropod fluxes varied by as

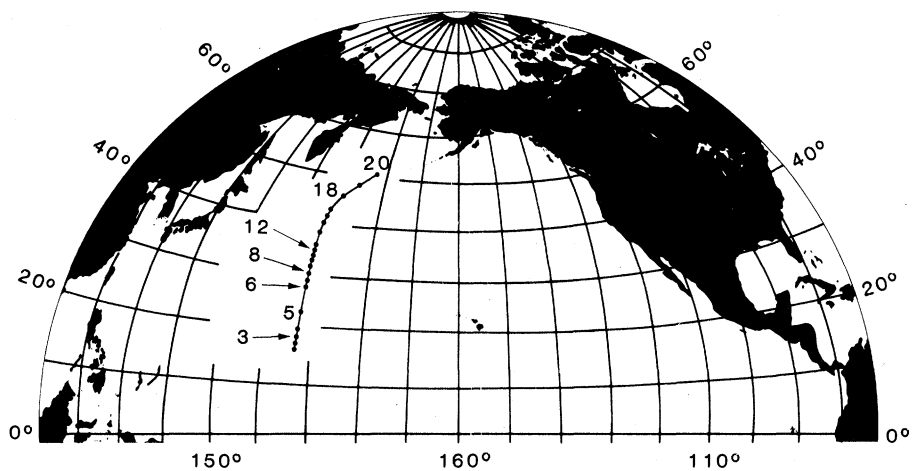


Fig. 1. Sediment trap stations for the North Pacific cruise of R/V *Discoverer* in May through June of 1982.

much as a factor of 15 and as little as 1.1 (Fig. 2), providing evidence of patchiness. When, however, the pteropod fluxes are converted to a percentage of the total mass flux in each trap, in all but one case (station 8) the proportion of pteropods in these samples is remarkably similar.

One of the major questions confronting geochemists studying the ocean's carbonate system is the dissolution patterns of biogenic carbonates. It has been assumed that for the calcitic foraminifera dissolution occurs principally after these organisms have settled to the sediment-water interface (19, 20). Although it has been suggested (20, 21) that pteropods also dissolve at the sediment-water interface, our data (Figs. 2 and 3) indicate that only a very small portion (about 10 percent) of the aragonite leaving the euphotic zone (upper 100 m) of the North Pacific settles deeper than 2200 m. The average flux of aragonite noted on this transect at 100 m was 30 mg m⁻² day⁻¹ compared to 0.9 mg m⁻² day⁻¹ at 2200 m. The average loss in the upper 2.2 km of the North Pacific was in excess of 90 percent ($\bar{X} = 93 \pm 8$). These results are supported by dissolution experiments carried out on the same cruise (13), which suggest that the smaller adult pteropods and juveniles which dominate our flux estimates are dissolved in the water column. In contrast, most of the CaCO₃ in large, rapidly settling species such as *Cuvierina columnella* is mobilized after reaching the bottom.

In marked contrast to most earlier work, Berner (20, 22) underscored the importance of aragonitic pteropods to the oceanic CO₂ system. Our observed pteropod/foraminifera (P/F) flux ratios are, however, even larger than Berner's estimates (P/F ≈ 1). We detected a P/F ratio at 100 m of <1 at only one location

(50°N). Furthermore, the ratios from the warm-water sphere in the North Pacific suggest that an average mass ratio for these classes of organisms is probably in excess of 5/1. The ratio is still considerably less than estimates (18) of relative P/F standing crops, 10/1. Although these mass ratios are far greater than earlier estimates (20, 22, 23), they are similar to those noted on a transect between 42° and 10°N along 155°W in the central Pacific in June 1981 (24). In addition, large fluxes of pteropods were noted on a transect of the equator (between 10°N and 6°S) along 150°W in January and February 1982 (15). Thus the data from seven stations in the western Pacific, six stations in the central Pacific, and four stations on an equatorial transect all show large masses of pteropods fluxing through the upper reaches of the Pacific.

Because of the marked difference in saturation state for aragonite and calcite in the North Pacific, it is possible to predict that with increasing depth there should be a marked decrease in the pteropod flux relative to the foraminifera flux. For the three stations where data are complete (stations 5, 8, and 12), the trends for the field data are in qualitative agreement with the prediction. At 21°N the P/F ratio at 2200 m is reduced to 31 percent of its value at 100 m, at 30°N to 10 percent, and at 35°N to 18 percent. In all cases, the more labile pteropods are being recycled considerably faster than the more stable foraminifera.

In addition to the systematic variation with depth, consistent latitudinal variations (about 40-fold) in the P/F mass ratio were noted at the base of the euphotic zone (100 m). The P/F ratio was highest in the southern areas, ≈20/1 at 21° and 30°N, decreased to 1.1 in the Kuroshio Extension, and reached a minimum value of 0.5 at our northernmost station

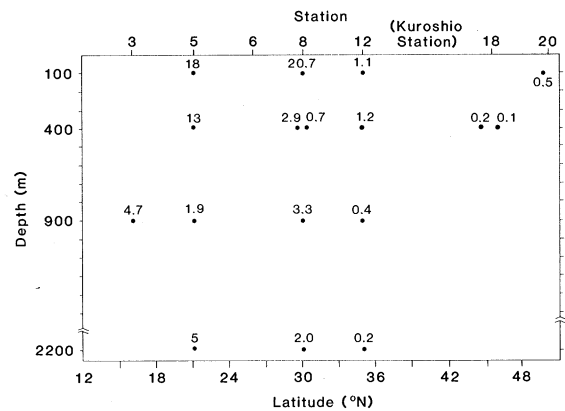
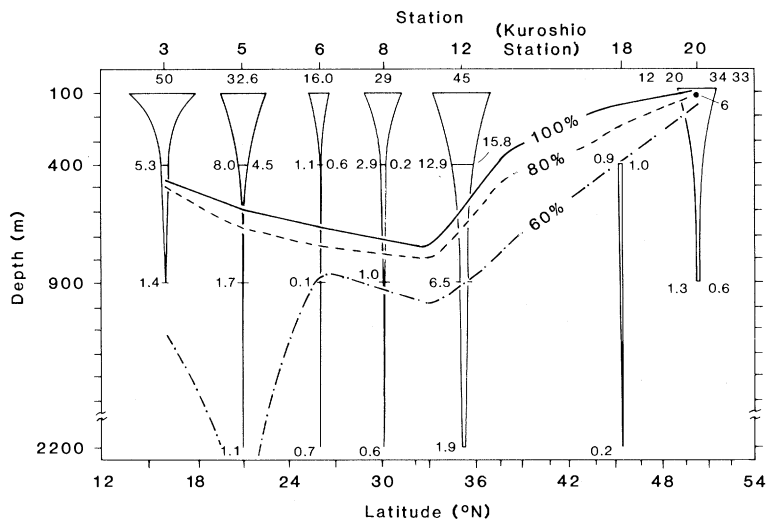


Fig. 2 (left). Depth distributions of pteropod fluxes (in milligrams per square meter per day) from the western North Pacific. Aragonite saturation state is shown for 100 percent saturation (—), 80 percent saturation (-----), and 60 percent saturation (-·-·-). Calculated fluxes do not

include small (≤ 10 percent) contributions from pteropod fragments.

Fig. 3 (right). Depth distribution for the mass flux ratio of aragonitic

(Fig. 3). Our absolute flux rates show that foraminifera were more abundant in the northern areas whereas pteropods dominated in the southern areas. Seasonal variations may alter this latitudinal trend, but our results indicate that net tows or sediment-trap collections made in one area of the North Pacific cannot be used for making basinwide estimates of the relative abundance of these organisms.

Few carbonate flux data are available for comparison with our work. In the investigation of Betzer *et al.* (15), mass fluxes were not partitioned into calcitic and aragonitic contributions. The total calcium fluxes reported by Tsunogai *et al.* (10) provide an upper-bound estimate for carbonate fluxes but no estimate of the relative importance of calcite and aragonite. Only the reports of Honjo (8) and Berner and Honjo (23) provide data for direct comparison with our results. In these investigations contributions of calcitic foraminifera were found to substantially dominate the total carbonate mass flux. The great difference between our results and earlier work (8, 23), in which aragonite is a relatively minor component of the total flux, is attributable to differences in collection procedures. In undersaturated water labile phases will dissolve continuously, and in the Pacific Ocean earlier collections made at 15°N, 153°W (8, 9) and 48°N, 176°E (10) were carried out for extended periods in undersaturated water. In the course of long collection times, 31 and 62 days (8–10) in undersaturated water, substantial aragonite dissolution should occur subsequent to sample collection. As an example, for 2000-m depths along our transect, model calculations based on shipboard dissolution analyses (13) predict

dissolution losses of at least 4 percent per day and as much as 14 percent per day. In addition, substantial losses of organic matter occur in sediment traps over short time scales (25). As a result, seawater in contact with trapped materials may become acidified (25) and undersaturated. In view of the large proportion of organic material associated with the large particle flux in shallow and intermediate waters (26), organic transformations may be an important means of dissolving aragonite phases during collection.

An interesting comparison can be made between our data and the alkalinity balance of the Pacific Ocean. The CO_2 /alkalinity model of Fiadeiro (12) indicated an average alkalinity input to intermediate and deep waters of the Pacific Ocean equivalent to a carbonate flux of $35 \text{ mg m}^{-2} \text{ day}^{-1}$. Recent calculations based on dissolved calcium concentrations in the western north Pacific suggest a carbonate dissolution flux of $63 \text{ mg m}^{-2} \text{ day}^{-1}$ (27). Our determinations of aragonite fluxes through the base of the euphotic zone (100 m) average $30 \pm 11 \text{ mg m}^{-2} \text{ day}^{-1}$. Apparently a portion of the substantial mass of large pteropods, excluded in our mass flux calculations, contributes to the carbonate dissolution flux of the North Pacific. Foraminiferal fluxes noted in this study and earlier work in the Pacific (9) fall far short of providing the necessary alkalinity flux to balance the model. However, at all five stations (Fig. 2) where traps were deployed at 100 and 400 m there were marked reductions in aragonite fluxes in supersaturated water. Although we are unable to resolve the processes that contribute to this unusual feature of our data, a variety of physical, chemical, and

biological processes can be proposed as possible explanations. Freshly exposed (1 to 3 days old) aragonite surfaces are significantly more soluble than aged aragonite surfaces (30 to 70 days old) (16, 28). If shells falling through the oceanic water column react as nonequilibrium phases (that is, are characterized by a greater apparent solubility product), then the aragonite saturation horizons in the North Pacific would be displaced toward the surface. In addition, diel migrations are an integral and well-defined characteristic of the oceanic biosphere (29). The possible relevance of this process to the CO_2 system arises from the possibility that organisms that feed on pteropods during evening and predawn hours might move deeper in the water column before defecating shells or alkaline fluids, or both. If, prior to defecation, some of these organisms and their carbonate baggage moved below the 400-m horizon, this would decrease the carbonate flux measured at 400 m and deliver alkalinity in the form of shells or fluids to intermediate depths. Additional laboratory and field work will be required to assess the relative importance of such physical-chemical and biological influences on the ocean's CO_2 system.

P. R. BETZER
R. H. BYRNE
J. G. ACKER
C. S. LEWIS
R. R. JOLLEY

Department of Marine Science,
University of South Florida,
St. Petersburg 33701

R. A. FEELY
Pacific Marine Environmental
Laboratory, National Oceanic and
Atmospheric Administration,
Seattle, Washington 98115

References and Notes

- R. Revelle and H. Suess, *Tellus* **9**, 18 (1959); B. Bolin and E. Ericksson, in *The Atmosphere and the Sea in Motion*, Rossby Memorial Volume, B. Bolin, Ed. (Rockefeller Institute Press, New York, 1959), p. 130; W. S. Broecker, T. Takahashi, H. J. Simpson, T.-H. Peng, *Science* **206**, 409 (1979).
- R. M. Rotty, in *The Fate of Fossil Fuel CO₂ in the Oceans*, N. Andersen and A. Malahoff, Eds. (Plenum, New York, 1977), p. 167; R. Rotty and G. Marland [Document ORAM-IEA-80-9(M), Institute for Energy Analysis, Oak Ridge Associated Universities, Oak Ridge, Tenn., 1980].
- J. Hansen *et al.*, *Science* **213**, 957 (1981); M. C. MacCracken, *ibid.* **220**, 873 (1983); J. Hansen *et al.*, *ibid.*, p. 874.
- T. Takahashi, W. S. Broecker, A. E. Bainbridge, R. F. Weiss, "Carbonate chemistry of the Atlantic, Pacific, and Indian oceans: Results of the GEOSECS Expedition 1972-1978" (Technical Report No. ICU-1-8, Lamont-Doherty Geological Observatory, Palisades, N.Y., 1980).
- C. Culberson and R. M. Pytkowicz, *Limnol. Oceanogr.* **13**, 403 (1968).
- C. Mehrbach, C. Culberson, J. E. Hawley, R. M. Pytkowicz, *ibid.* **18**, 897 (1973).
- F. J. Millero, *Geochim. Cosmochim. Acta* **43**, 1651 (1979).
- S. Honjo, *J. Mar. Res.* **38**, 53 (1980).
- R. C. Thunell and S. Honjo, *Mar. Geol.* **40**, 237 (1981).
- S. Tsunogai, M. Uematsu, S. Noriki, N. Tanaka, M. Yamada, *Geochim. J.* **16**, 129 (1982).
- R. A. Feely and C. T. A. Chen, *Geophys. Res. Lett.* **9**, 1294 (1982); R. A. Feely, R. H. Byrne, P. R. Betzer, J. F. Gendron, J. G. Acker, *J. Geophys. Res.*, in press.
- M. Fiadeiro, *Earth Planet. Sci. Lett.* **49**, 499 (1980).
- R. H. Byrne, J. G. Acker, P. R. Betzer, R. A. Feely, M. Cates, *Nature (London)*, in press.
- A. Soutar, S. A. Kline, E. Duffrin, K. W. Bruland, *Nature (London)* **266**, 136 (1977).
- P. R. Betzer *et al.*, *Deep Sea Res.* **31**, 1 (1984).
- J. W. Morse, A. Mucci, F. W. Millero, *Geochim. Cosmochim. Acta* **44**, 85 (1980).
- A. W. H. Bé and R. W. Gilmer, *Oceanic Micropaleontology*, A. T. S. Ramsay, Ed. (Academic Press, New York, 1977), p. 733.
- J. A. McGowan, in *The Micropaleontology of Oceans*, B. M. Funnell and W. R. Riedel, Eds. (Cambridge Univ. Press, Cambridge, 1971), p. 3; in *The Biology of the Oceanic Pacific*, C. B. Miller, Ed. (Proceedings of the 33rd Annual Biology Colloquium) (Oregon State Univ. Press, Corvallis, 1974), p. 9; J. L. Reid, E. Brinton, A. Fleminger, E. L. Venrick, J. A. McGowan, in *Advances in Oceanography*, H. Charnock and G. Deacon, Eds. (Plenum, New York, 1978), p. 65.
- W. H. Berger, C. G. Adelseck, L. A. Mayer, *J. Geophys. Res.* **81**, 2617 (1976).
- R. A. Berner, *The Fate of Fossil Fuel CO₂ in the Oceans*, N. Andersen and A. Malahoff, Eds. (Plenum, New York, 1977), p. 243.
- S. Honjo, *ibid.*, p. 269.
- R. A. Berner, *Ambio Special Rep. No. 6* (1979), p. 5.
- _____ and S. Honjo, *Science* **211**, 940 (1981).
- P. R. Betzer, R. H. Byrne, R. A. Feely, *Eos* **63** (No. 3), 45 (1982) (abstract).
- W. D. Gardner, K. R. Hinga, J. Marra, *J. Mar. Res.* **41**, 195 (1983).
- J. K. Bishop, J. M. Edmond, D. R. Ketten, M. P. Bacon, W. B. Silker, *Deep Sea Res.* **24**, 511 (1977); D. A. Fellows, D. M. Karl, G. A. Knauer, *ibid.* **28**, 921 (1981).
- S. Tsunogai and Y. Watanabe, *Geochim. J.* **15**, 95 (1981).
- I. N. Plummer and E. T. Sundquist, *Geochim. Cosmochim. Acta* **46**, 247 (1982).
- A. C. Hardy, in *The Open Sea. Its Natural History: The World of Plankton* (Collins, London, 1956); I. A. MacLaren, *J. Fish. Res. Board Can.* **20** (No. 3), 685 (1963); M. F. Vinogradov, in *The Vertical Distribution of the Oceanic Zooplankton* (Publication TT-69-59015, National Technical Information Service, Springfield, Va., 1970).
- We thank Captain R. Speer and the crew of the R.V. *Discoverer*, who were especially effective throughout the cruise. We owe a special tribute to Chief Bosun W. Sherril and the deck crew whose hard and competent work made possible multiple launchings and retrievals of the free-drifting sediment traps. We thank J. Cline who was always prepared to solve problems and D. Jones and A. King who provided logistical help prior to the cruise. We express special thanks to J. A. McGowan for encouragement and help with this project. This research was supported by a grant from the Air Resources Laboratory under the direction of L. Machta to the University of South Florida (NA80RAD00020). Contribution No. 735 from Pacific Marine Environmental Laboratory.

29 June 1984; accepted 14 September 1984

Activation of the *c-myb* Locus by Viral Insertional Mutagenesis in Plasmacytoid Lymphosarcomas

Abstract. *Rearrangement in the c-myb locus of each of four independently derived BALB/c plasmacytoid lymphosarcoma (ABPL's) is due to the insertion of a defective Moloney murine leukemia virus (M-MuLV) into a 1.5-kilobase-pair stretch of cellular DNA at the 5' end of the v-myb-related sequences. This retroviral insertion is associated with abnormal transcription of myb sequences and probably represents a step in the neoplastic transformation of ABPL cells.*

Three types of B lymphocytic tumors arise in BALB/c mice after they receive intraperitoneal injections of pristane and Abelson virus. On the basis of their morphology and association with Abelson virus these tumors are termed lymphosarcomas (ABLS's), plasmacytomas (ABPC's), and plasmacytoid lymphosarcomas (ABPL's) (1). The Abelson virus used in the tumor induction contained two retroviral elements: the replication-defective, transforming Abelson murine leukemia virus (A-MuLV) and the transmissible helper Moloney murine leukemia virus (M-MuLV). Both viral elements have the same 5' and 3' ends of the viral genome, including two long

terminal repeats (LTR's). The central portion of the M-MuLV gene has been replaced by the transforming *v-abl* sequence in A-MuLV (2). All ABLS's and ABPC's contain integrated A-MuLV proviral genomes and synthesize abundant *v-abl* RNA, while ABPL's do not (1). Instead, each of the ABPL's has undergone a DNA rearrangement in one of the *c-myb* loci, resulting in the synthesis of abnormal messenger RNA transcripts (1). Because *c-myb* is the cellular homolog of viral *myb* (*v-myb*) of avian myeloblastosis virus (AMV) and because the *v-myb* sequence is thought to be essential for the oncogenic properties of AMV in certain target cells (3), the dis-

ruption of the *c-myb* locus and transcription of an altered form of *c-myb* in ABPL's could result in the induction, progression, or maintenance of these tumors.

In elucidating the mechanism by which the *c-myb* locus is rearranged in the ABPL's, the *c-myb* locus of four ABPL's was first examined at the DNA level. Normal BALB/c liver and ABPL DNA's were digested with Eco RI and analyzed by the method of Southern (4) (Fig. 1). The DNA's were first probed (Fig. 1A) with the avian *v-myb* sequence isolated as a 1.3-kilobase-pair (kbp) Kpn I-Xba I fragment from a chicken AMV proviral clone (5, 6). In addition to the 4.2-, 2.0-, 1.7-, and 1.5-kbp *myb* hybridizing bands in normal BALB/c liver DNA, each of the four ABPL's contained a larger band of varying size. In experiments to determine which part of the *c-myb* locus was altered, a 0.5-kbp Kpn I-Eco RI fragment which represents the 5' half of the *v-myb* was isolated from a chicken AMV provirus clone (λ 11A-1-1) (6). When this was used as a probe, only the 4.2-kbp band and the rearranged *myb* bands showed hybridization (Fig. 1B). This indicates that the 4.2-kbp Eco RI fragment contained the portion of *c-myb* homologous with the 5' *v-myb* region and that this fragment was altered in the ABPL's, giving rise to the larger Eco RI fragments. Furthermore, when the DNA's were probed with a 0.8-kbp Eco RI-Xba I fragment which represents the 3' half of the *v-myb* sequence, only the smaller bands but not the 4.2-kbp or the rearranged Eco RI fragments showed hybridization (data not shown). Hence, the rearrangement had occurred at the 5' end of the *c-myb* locus in each of these four ABPL's. Presumably, it is this rearrangement in the *c-myb* locus in ABPL's that results in the synthesis of the larger *myb* RNA transcripts that have been described (1).

To study the altered *myb* locus in ABPL's, we cloned these sequences from Eco RI-digested genomic DNA's from four of the ABPL's with the use of λ gt WES \cdot λ B vectors (7). The recombinant λ clones were selected by hybridization with *v-myb*. Unrearranged *c-myb* sequences were also obtained by screening a bacteriophage library of BALB/c mouse DNA (partial Eco RI* digest). The Eco RI insert from each of these clones was subcloned in pBR322 and used in all subsequent studies.

For elucidation of the molecular nature of the DNA rearrangement, the 7.5-kbp Eco RI insert from ABPL2 was hybridized to the corresponding 4.2-kbp Eco RI fragment of the normal *c-myb*